

Supporting Information

An Aqueous Aluminum-Ion Electrochromic Full Battery

Zhongqiu Tong, Ruqian Lian, Rui Yang, Tianxing Kang, Jianrui Feng, Dong Shen, Yan Wu,
Xiao Cui, Hui Wang, Yongbing Tang and Chun-Sing Lee*

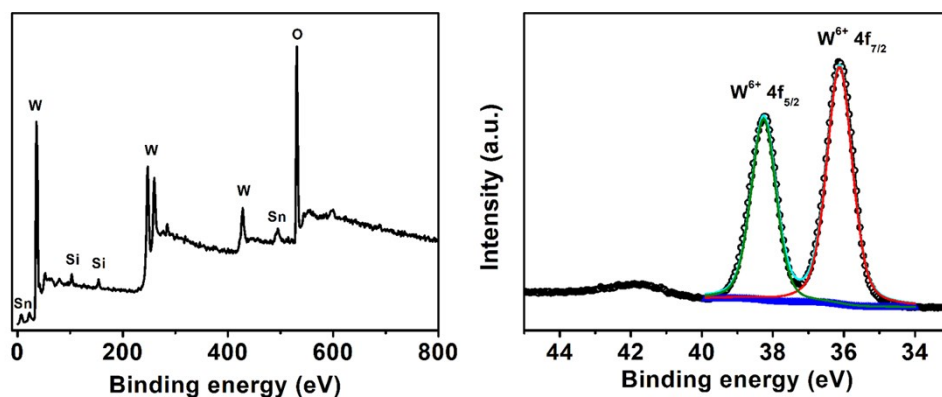


Figure S1. (a) XPS spectrum of the prepared a-WO₃ film. (b) W 4f XPS spectrum of the prepared a-WO₃ film. Si and Sn signals are from the FTO substrate.

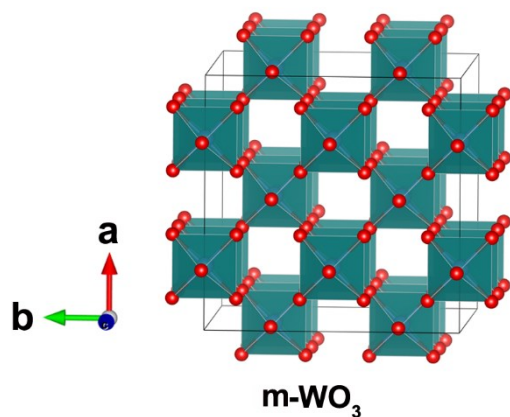


Figure S2. Crystalline lattice of the m-WO₃.

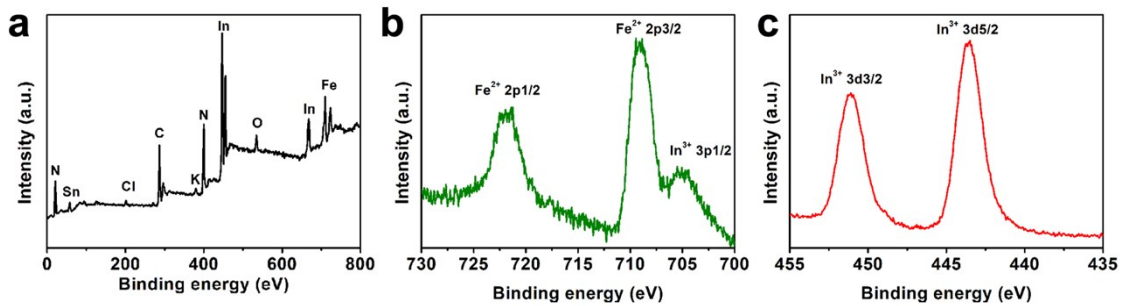


Figure S3. (a) Survey scan; (b) Fe 2p; and (c) In 3d XPS spectra of the as-prepared InHCF film.

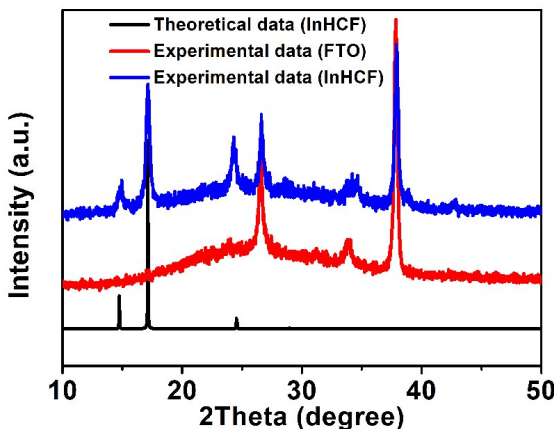


Figure S4. Experimental and simulated XRD patterns of the as-prepared InHCF sample.

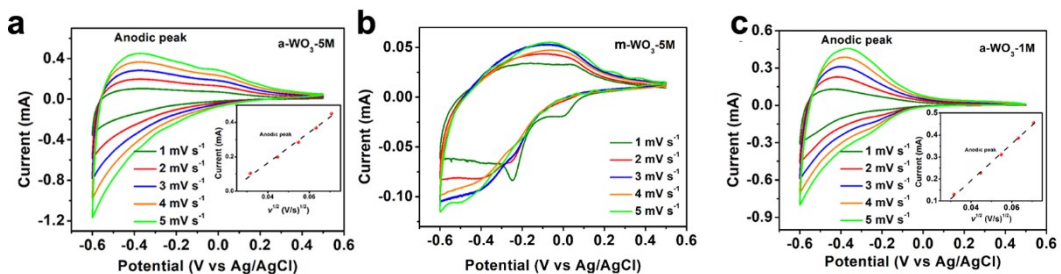


Figure S5. (a) CV profiles of a-WO₃ film in 5 M electrolyte at various scan rates. (b) CV profiles of m-WO₃ film in 5 M electrolyte at various scan rates. (c) CV profiles of a-WO₃ film in 1 M electrolyte at various scan rates.

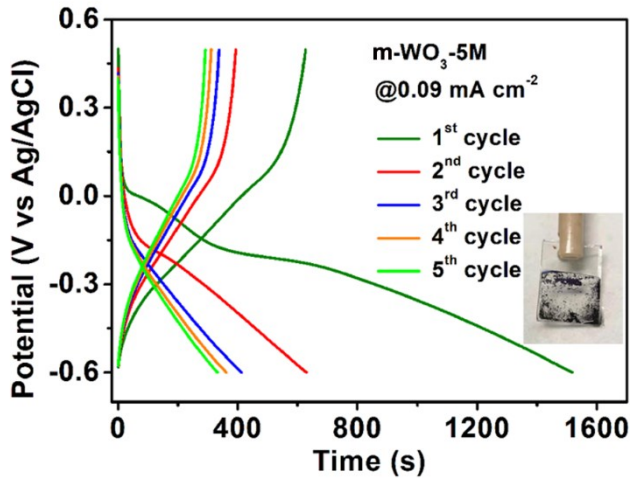


Figure S6. Charge/discharge profiles of m-WO₃ film in 5 M electrolyte at 0.09 mA cm⁻². Inset photo demonstrating the film integrity after 5 cycles at 0.09 mA cm⁻².

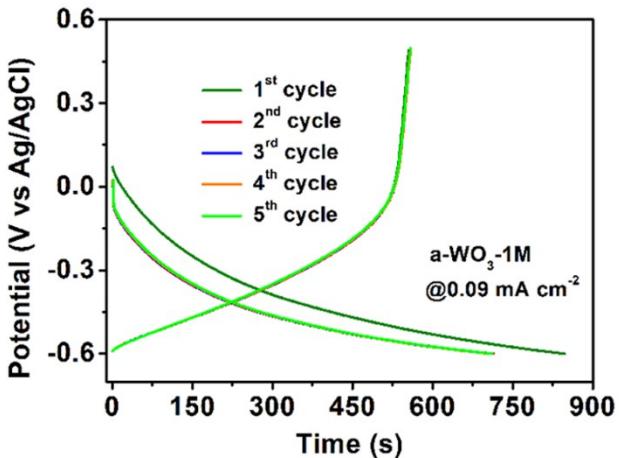


Figure S7. Charge/discharge profiles of the a-WO₃ film in 1 M electrolyte at 0.09 mA cm⁻².

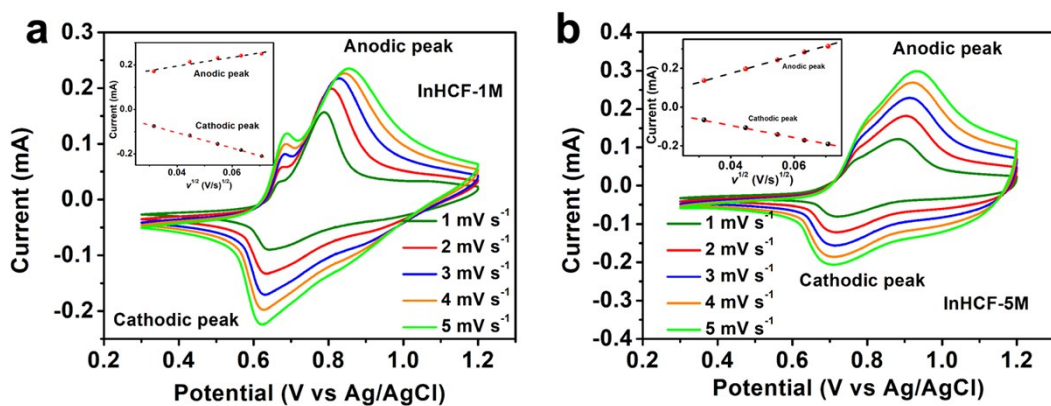


Figure S8. (a) CV profiles of the InHCF film in 1 M electrolyte at various scan rates. (b) CV profiles of the InHCF film in 5 M electrolyte at various scan rates. The inset curves are the fitting plots to calculate the $D_{\text{Al-ion}}$ values demonstrating the influence of Al(OTF)₃ concentrations on the redox kinetics.

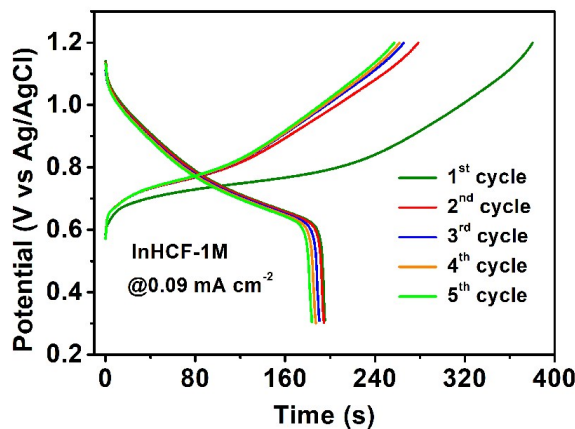


Figure S9. Charge/discharge profiles of the InHCF film in 1 M electrolyte at 0.09 mA cm^{-2} .

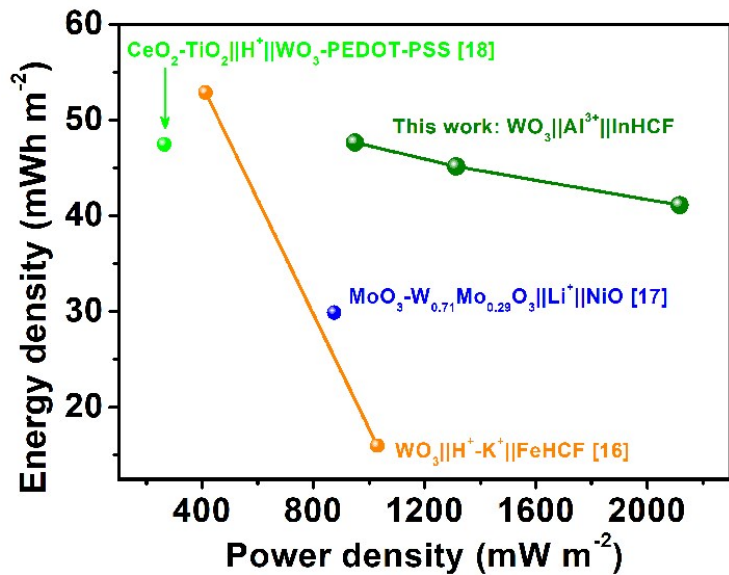


Figure S10. Comparison about the energy and power densities between assembled AAEFB and typically reported electrochromic full batteries. The structures of cells are demonstrated by the components of cathode material, anode material and the shuttling charge carrier.

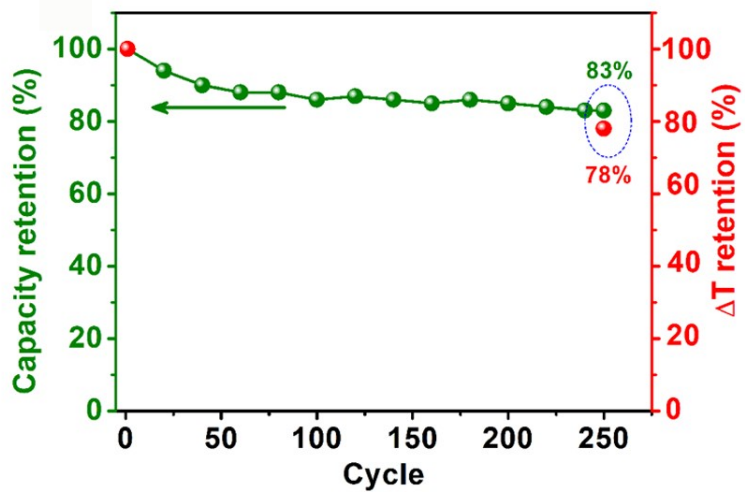


Figure S11. Cycling stability of discharge capacity and transmittance modulation of AAEFB at 0.15 mA cm^{-2} for 250 cycles.

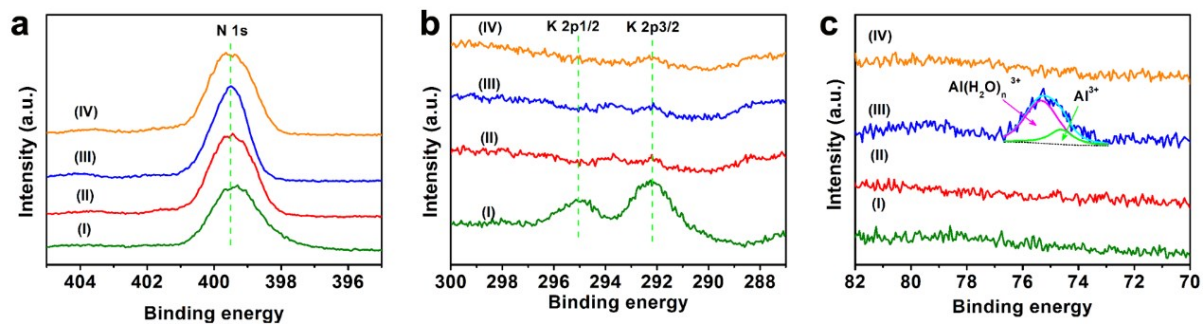


Figure S12. (a) *Ex situ* XPS spectra recorded from N 1s of the InHCF film during the initial charge/discharge/charge process. (b) *Ex situ* XPS spectra recorded from K 2p of the InHCF film during the initial charge/discharge/charge process. (c) *Ex situ* XPS spectra recorded from Al 2p of the InHCF film during the initial charge/discharge/charge process. Deconvolution about the Al 2p spectrum of fully discharged state (state III) is conducted to analyze inserted Al-ion types.

Table S1. Comparison on the average discharge voltage of reported aqueous electrochromic multivalent-ion batteries with metal anodes (Ref. 1 to Ref. 12) and aqueous non-electrochromic Al-ion full cells (Ref. 13 to Ref. 15).

Anode	Cathode	Electrolyte	Average discharge voltage (V)	Reference
Zn	Mo/Ti:WO ₃ (MTWO)	1 M ZnSO ₄ solution	0.32	[1]
Zn	V ₃ O ₇	1 M ZnSO ₄ solution	0.8	[2]
Zn	Polypyrrole (PPy)	PVA/KCl/Zn(CH ₃ COO) ₂ gel electrolyte	0.57	[3]
Zn	Viologen	1 M ZnSO ₄ solution	0.34	[4]
Zn	Self-doped polyaniline (SPANI)	PVA/Zn(CF ₃ SO ₃) ₂ gel	0.96	[5]
Zn	WO ₃	DMSO-ZnSO ₄ /AlCl ₃ hydrogel electrolyte	0.65	[6]
Zn	WO ₃	1 M ZnSO ₄ solution	0.42	[7]
Zn	WO ₃	1 M ZnSO ₄ / 1M AlCl ₃ solution	0.29	[7]
Mg	Prussian blue	1 M KCl, 0.1 M phosphate buffer (pH 6), and 4 mM NaClO solution	0.21	[8]
Al	Prussian blue	3 M KCl solution	0.92	[9]
Al	WO ₃	1 M AlCl ₃ solution	0.28	[10]
Al	Polypyrrole (PPy)	3 M KCl solution	0.38	[11]
Al	WO ₃	1 M AlCl ₃ solution	0.32	[12]
MoO ₃	CuHCF	Al(NO ₃) ₃ -PVA gel electrolyte	0.47	[13]
MoO ₃	VOPO ₄ •2H ₂ O	Al(NO ₃) ₃ -gelatin-PAM hydrogel electrolyte	0.47	[14]
Activated carbon	K _{0.02} Cu[Fe(CN) ₆] _{0.7} •3.7H ₂ O	1 M Al(NO ₃) ₃ solution	0.52	[15]
WO ₃	InHCF	5M Al(OTf) ₃ solution	0.93@0.10 mA cm ⁻² 0.85@0.25 mA cm ⁻²	This work

Reference:

- [1] H. Li, L. McRae, C. Firby, A. Elezzabi, Adv. Mater., 2019, 31, 1807065.
- [2] W. Zhang, H. Li, M. Al-Hussein, A. Elezzabi, Adv. Optical Mater., 2020, 8, 1901224.
- [3] J. Wang, J. Liu, M. Hu, J. Zeng, Y. Mu, Y. Guo, J. Yu, X. Ma, Y. Qiu, Y. Huang, J. Mater. Chem. A, 2018, 6, 11113.
- [4] C. Wang, Z. Wang, Y. Ren, X. Hou, F. Yan, ACS Sustainable Chem. Eng., 2020, 8, 5050.
- [5] Y. Wang, H. Jiang, R. Zheng, J. Pan, J. Niu, X. Zou, C. Jia, J. Mater. Chem. A, 2020, 8, 12799.
- [6] H. Eric, H. Li, A. Elezzabi, RSC Adv., 2019, 9, 32047.
- [7] H. Li, C. Firby, A. Elezzabi, Joule, 2019, 3, 2268.
- [8] Y. Zhai, Y. Li, H. Zhang, D. Yu, Z. Zhu, J. Sun, S. Dong, ACS Appl. Mater. Interfaces, 2019, 11, 28072.

- [9] J. Wang, L. Zhang, L. Yu, Z. Jiao, H. Xie, X. Lou, X. Sun, *Nat. Comm.* 2014, 5, 4921.
- [10] J. Zhao, Y. Tian, Z. Wang, S. Cong, D. Zhou, Q. Zhang, M. Yang, W. Zhang, F. Geng, Z. Zhao, *Angew. Chem. Int. Ed.*, 2016, 55, 7161.
- [11] B. Yang, D. Ma, E. Zheng, J. Wang, *Sol. Energy Mater. Sol. Cells*, 2019, 192, 1.
- [12] S. Sun, C. Tang, Y. Jiang, D. Wang, X. Chang, Y. Lei, N. Wang, Y. Zhu, *Sol. Energy Mater. Sol. Cells*, 2020, 207, 110332.
- [13] P. Wang, Z. Chen, Z. Ji, Y. Feng, J. Wang, J. Liu, M. Hu, H. Wang, W. Gan, Y. Huang, *Chem. Eng. J.* 2019, 373, 580.
- [14] P. Wang, Z. Chen, H. Wang, Z. Ji, Y. Feng, J. Wang, J. Liu, M. Hu, J. Fei, W. Gan, *Energy Storage Mater.*, 2020, 25, 426.
- [15] Z. Li, K. Xiang, W. Xing, W. Craig Carter, Y. Chiang, *Adv. Energy Mater.*, 2015, 5, 1401410.
- [16] L. Chen, K. Tseng, Y. Huang, K. Ho, *J. New Mat. Electrochem. Systems*, 2002, 5, 213.
- [17] H. Lia, L. McRae, C. Firby, M. Al-Hussein, A. Elezzabi, *Nano Energy*, 2018, 47 130.
- [18] G. Cai, P. Darmawan, X. Cheng, P. Lee, *Adv. Energy Mater.*, 2017, 7, 1602598.